Journal of Physics: Conference Series

PAPER • **OPEN ACCESS**

Remote pipeline assessment and condition monitoring using low-frequency axisymmetric waves: a theoretical study of torsional wave motion

To cite this article: J M Muggleton *et al* 2016 *J. Phys.: Conf. Ser.* **744** 012055

Remote pipeline assessment and condition monitoring using low-frequency axisymmetric waves: a theoretical study of torsional wave motion

J M Muggleton[1], E Rustighi[1] & Y Gao[1,2]

[1]Institute of Sound & Vibration Research, University of Southampton, Highfield, Southampton, UK
[2]Key laboratory of Noise and Vibration Research Institute of Acoustics, Chinese Academy of Sciences (IACAS) Beijing 100190 China

jmm@isvr.soton.ac.uk

Abstract. Waves that propagate at low frequencies in buried pipes are of considerable interest in a variety of practical scenarios, for example leak detection, remote pipe detection, and pipeline condition assessment and monitoring. Particularly useful are the n=0, or axisymmetric, modes in which there is no displacement (or pressure) variation over the pipe cross section. Previous work has focused on two of the three axisymmetric wavetypes that can propagate: the s=1, fluid-dominated wave; and the s=2, shell-dominated wave. In this paper, the third axisymmetric wavetype, the s=0 torsional wave, is studied. Whilst there is a large body of research devoted to the study of torsional waves and their use for defect detection in pipes at ultrasonic frequencies, little is known about their behaviour and possible exploitation at lower frequencies. Here, a low-frequency analytical dispersion relationship is derived for the torsional wavenumber for a buried pipe from which both the wavespeed and wave attenuation can be obtained. How the torsional waves subsequently radiate to the ground surface is then investigated, with analytical expressions being presented for the ground surface displacement above the pipe resulting from torsional wave motion within the pipe wall. Example results are presented and, finally, how such waves might be exploited in practice is discussed.

1. Introduction

Much attention has recently been paid to remotely detecting buried pipes and cables in all ground conditions without the need for excavation, under the umbrella of a major UK initiative entitled "Mapping the Underworld" (MTU) [1]. Building on the highly successful outcomes from MTU, A new research project, entitled "Assessing the Underworld" (ATU) [2], has recently commenced to take the research into a new sphere. This programme aims to use geophysical sensors deployed both on and beneath the ground surface to remotely determine the condition of urban assets. One of the four essential technologies in the MTU, vibro-acoustics, has been proven to be suitable and highly successful for locating buried water pipes [3,4]. In the ATU phase, some of the vibro-acoustic techniques developed in MTU will be extended from detecting pipes to assessing their condition. It is within this framework that the work presented here has been undertaken.

Failures in aging water mains are a serious problem for all water distribution systems. There has been considerable research and commercial attention on the accurate location of water leakage for many years [5-7], but the various causes of pipe failures, and their identification, have not been well documented;

moreover, there are still a number of gaps in the existing knowledge. One mode of failure, about which there is very little in either the academic or industrial literature, is spiral fracture, occurring, for the most part, in cast iron pipes [8]. Beyond the obvious case of a spirally welded pipe, it is not altogether clear what mechanism might underlie such a failure.

Perhaps more tractable is the link between spiral failure (however initiated) and the wave motion set up within the pipe in consequence. There is a desire to be able to detect and locate fracture events as they occur and, if possible, remotely confirm the likely mode of failure. For a vibro-acoustic technique to be effective, the acoustic characteristics of the dominant wave mode(s) associated with particular types of pipe failure must be known *a priori*. Furthermore, how these waves may radiate to the ground surface, where than can potentially be detected, is of considerable interest. In general, in buried water pipes, acoustic energy propagates at relatively low frequencies [9]. Of the four main energy carriers, three of them are axisymmetric (n=0) waves including a predominantly fluid-borne (s=1) wave, a compressional shell (s=2) wave, and a torsional (s=0) wave. Much of the present authors' previous work has involved both theoretical and experimental investigations into the s=1, 2 waves [10-14]. The focus of the present paper is the s=0, torsional wave. Whilst, in the field, it has not been confirmed beyond reasonable doubt, it would seem logical to assume that, when a spiral fracture occurs in a pipe, torsional waves are excited and thence propagate along the pipe. Moreover, if it were possible to detect these waves from the ground surface, possibilities for the remote detection and monitoring of the fracture events open up.

Torsional waves in pipes have received considerable attention in the literature at ultrasonic frequencies to support commercial testing systems that have been in use in industry for a number of years. They are exploited for the detection and characterization of cracks and other (small) pipe defects in both unburied and buried pipe, for example[15-22]. At these high frequencies, the fundamental torsional wave in a buried pipe is non-dispersive, propagating at the same speed as that in an *in-vacuo* pipe. Little is available in the literature for the low-frequency regime, beyond the *in vacuo*, textbook solution. To the authors' knowledge nothing has, to date, been presented on the low-frequency behaviour of buried pipes and the concomitant response within the soil, in particular, in terms of an analytical solution. In this paper, the dispersion characteristics of the fundamental torsional wave in a buried pipe at low (typically <1 kHz) frequencies is studied and analytical solutions presented. Additionally, the resultant response within the surrounding ground is examined.

The present paper is organized as follows: In section 2, the equations of motion are derived, leading to the dispersion relationship for torsional motion; an analytical expression for the torsional wavenumber is presented, which encapsulates both the wavespeed and the wave attenuation. In Section 3, how such waves might radiate to the ground surface is considered; an approximate analytical expression for the displacement seen at the ground surface relative to the circumferential motion of the pipe wall is derived; this in turn can be related to the circumferential pipe wall motion at any point along its length. In Section 4, numerical examples are presented for a cast iron pipe; two typical soil types are considered. Finally, some practical applications of this research are considered and conclusions presented.

2. Dispersion relationship for the *n*=0, *s*=0, torsional wave

The pipe equations for $n = 0$ axisymmetric, torsional wave motion are derived for a buried fluid-filled pipe. The surrounding soil is regarded as an infinite elastic medium which can sustain both compressional and shear waves. A semi-infinite, isotropic, cylindrical shell is shown in Fig. 1: the shell displacements are u, v and w in the axial (x), circumferential (θ), and radial (r) directions, respectively; u_r, u_θ and u_x denote the soil displacements in the r, θ and x directions respectively. The contained fluid imposes a pressure (p_f) on the pipe wall; the surrounding soil imposes normal stress $\tilde{\sigma}_{rr}$ and tangential stresses $\tilde{\sigma}_{r\theta}$ and $\tilde{\sigma}_{rx}$ at the pipe/soil interface. The pipe has a mean radius a and wall thickness h, and is assumed to be thin such that $h << a$. The following are simplified forms of Kennard's equations for a thin-walled shell [23], with shell bending neglected, and so are only valid

below the ring frequency. The contained fluid is considered to be uncoupled from the pipe motion because a fluid cannot support shear.

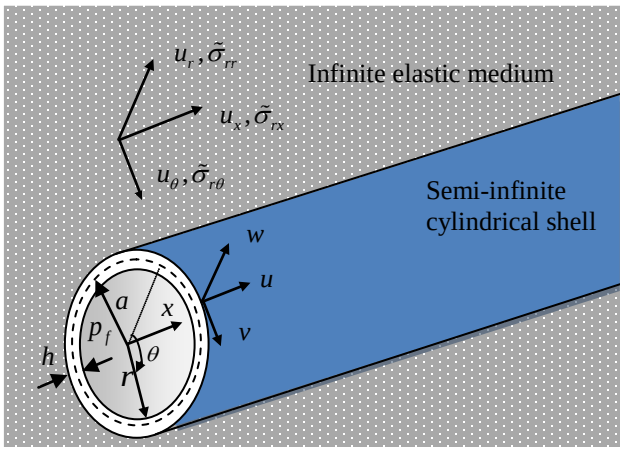

Fig. 1. The coordinate system for a buried, fluid-filled pipe

For axisymmetric torsional motion in the soil, u_q, assuming an axial travelling wave dependence, $u_\theta = V_m e^{\mathrm{i}(\omega t - k_0 x)}$, the equation of motion for V_m is given by

$$\frac{\partial^2 V_m}{\partial r^2} + \frac{\partial V_m}{r \partial r} - \frac{V_m}{r^2} + \left(k_{r0}^r\right)^2 V_m = 0 \tag{1}$$

where the soil shear (rotational) radial wavenumber k_{r0}^r is given by $(k_{r0}^r)^2 = k_r^2 - k_0^2$; and k_r is the shear wavenumber in the soil, which is given by $k_r^2 = \omega^2 \rho_m / \mu_m$. As expected, under these conditions, only a shear wave may exist in the surrounding soil. To represent an outgoing shear wave decaying to zero at infinity, a Hankel function of the second kind H_1 of order one is used to solve the Bessel's Eq. (1), $V_m = B\,\mathrm{H}_1\left(k_{r0}^r r\right)$ where B is a constant. Thus, the travelling wave solution becomes

$$u_\theta = B\,\mathrm{H}_1\left(k_{r0}^r r\right) e^{\mathrm{i}(\omega t - k_0 x)} \tag{2}$$

According to Hooke's Law, the tangential stress $\tilde{\sigma}_{r\theta}$ is given by

$$\tilde{\sigma}_{r\theta} = \mu \left[\frac{1}{r}\frac{\partial u_r}{\partial \theta} + r \frac{\partial}{\partial r}\left(\frac{u_\theta}{r}\right) \right] \tag{3}$$

Substituting the travelling wave solution of u_θ given by Eq. (8) into (9) (u_r=0) results in

$$\tilde{\sigma}_{r\theta}(r) = B\mu_m \left[k_{r0}^r\, \mathrm{H}_1'\left(k_{r0}^r r\right) - \frac{\mathrm{H}_1\left(k_{r0}^r r\right)}{r} \right] e^{\mathrm{i}(\omega t - k_0 x)} \tag{4}$$

where $\mathrm{H}_1'(\ ) = (\partial / \partial r)\mathrm{H}_1(\ )$.

For the shell, each cross-section remains in its own plane and rotates about the x axis. Noting that the

surrounding soil only exerts a tangential stress, $\tilde{\sigma}_{r\theta}(a)$, at the boundary $r=a$, equilibrium of forces in the circumferential direction gives

$$\rho_p \ddot{v} = \frac{\partial \sigma_{x\theta}}{\partial x} + \frac{\tilde{\sigma}_{r\theta}(a)}{h} \tag{5}$$

Exploiting Hooke's law for the shell gives the tangential stress $\sigma_{x\theta}$ as

$$\sigma_{x\theta} = G_p \left(1 + \frac{h}{a}\right) \frac{\partial v}{\partial x} \tag{6}$$

Where G_p is the shear modulus of the pipe wall material. Combining these two equations then gives

$$\rho_p \ddot{v} = G_p \left(1 + \frac{h}{a}\right) \frac{\partial^2 v}{\partial x^2} + \frac{\tilde{\sigma}_{r\theta}(a)}{h} \tag{7}$$

Similar to the soil displacements, a travelling wave solution of the form $v = V_s \mathrm{e}^{\mathrm{i}(\omega t - k_s x)}$ is used to describe the pipe wall displacement, where V_s is its amplitude in the circumferential direction.

The coefficient B in Eq. (4) may be determined from the conditions at the pipe/soil interface. Here we consider compact contact for which there is a no slip condition between the pipe wall and the soil - except when very large shear strains are expected, as might be the case for earthquake-excited motion, this condition is likely to be maintained. Thus Eq. (2) becomes

$$B = \frac{V_0}{\mathrm{H}_1(k_{r0}^r a)} \tag{8}$$

From Eq. (4) this then gives the shear stress at the pipe wall as

$$\tilde{\sigma}_{r\theta}(a) = \frac{V_s \mu_m}{a} \left[k_{r0}^r a \frac{\mathrm{H}_1'\left(k_{r0}^r a\right)}{\mathrm{H}_1\left(k_{r0}^r a\right)} - 1 \right] e^{\mathrm{i}(\omega t - k_0 x)} \tag{9}$$

For a thin walled pipe for which $h \ll a$, substituting into Eq. (7) and adopting the travelling wave solution for the pipe wall displacement, v, gives (after some manipulation) the torsional wavenumber as

$$k_0^2 = k_T^2 \left\{ 1 + \frac{\mu_m / a}{\omega^2 \rho_p h} \left[k_{r0}^r a \frac{\mathrm{H}_1'\left(k_{r0}^r a\right)}{\mathrm{H}_1\left(k_{r0}^r a\right)} - 1 \right] \right\} \tag{10}$$

where k_T is given by $k_T^2 = \omega^2 \rho_p / G_p$.

The individual terms contributing to the wavenumber expression can be readily identified as:

- the *in-vacuo* torsional wavenumber, k_T;
- a pipe wall mass component, $\omega^2 \rho_p h$;
- a soil shear stiffness component, μ_m/a;
- and a shear wave radiation component associated with the Hankel function ratio,

$$k_{r0}^{r} a \frac{\mathrm{H}_1'\left(k_{r0}^{r} a\right)}{\mathrm{H}_1\left(k_{r0}^{r} a\right)}$$

Eq. (10) can now be examined in a little more detail. In non-dimensional form, and substituting for ω it becomes

$$\left(k_0 a\right)^2 = \left(k_T a\right)^2 + \frac{\mu_m}{G}\frac{a}{h}\left[k_{r0}^{r} a \frac{\mathrm{H}_1'\left(k_{r0}^{r} a\right)}{\mathrm{H}_1\left(k_{r0}^{r} a\right)} - 1\right] \tag{11}$$

At high frequencies, when the asymptotic forms of the Hankel functions for large arguments can be used [24], Eq. (22) becomes

$$\left(k_0 a\right)^2 \approx \left(k_T a\right)^2 \left\{1 - \frac{\mu_m}{G}\frac{a}{h}\frac{1}{\left(k_T a\right)^2} k_{r0}^{r} a \exp^{\mathrm{i}\frac{\pi}{2}}\right\} \tag{12}$$

Taking the square root and retaining only the first two terms in the series expansion gives, after some manipulation

$$k_0 a \approx k_T a - \frac{\mathrm{i}}{2}\frac{\mu_m}{G}\frac{a}{h}\frac{k_{r0}^{r} a}{k_T a} \tag{13}$$

This shows that, at high frequencies, the real part of the *s*=0 wavenumber, related to the wavespeed, tends, as expected, to the *in vacuo* value. Substituting for $k_{r0}^{r} a$ using $(k_{r0}^{r})^2 = k_r^2 - k_0^2$ and approximating k_0 as k_T then gives the imaginary component of the *s*=0 wavenumber as

$$\mathrm{Im}\left\{k_0 a\right\} \approx \mathrm{Im}\left\{k_T a\right\} - \frac{1}{2}\frac{\mu_m}{G}\frac{a}{h}\sqrt{\frac{k_r^2}{k_T^2} - 1} \tag{14}$$

When the *in-vacuo* torsional wavespeed in the pipe is much greater than the shear wavespeed in the soil ($k_r^2 >> k_T^2$), Eq. (14) becomes

$$\mathrm{Im}\left\{k_0 a\right\} \approx \mathrm{Im}\left\{k_T a\right\} - \frac{1}{2}\frac{a}{h}\sqrt{\frac{\mu_m}{G}}\sqrt{\frac{\rho_m}{\rho_p}} \tag{15}$$

It can be seen that the imaginary part of the wavenumber comprises two terms: one associated with losses within the pipe wall; and the second associated with radiation losses. When the pipe wall losses are small, such as is the case for metal pipes, the imaginary part of the pipe wavenumber becomes a constant. It is also clear now that the pipe does not simply become uncoupled from the surrounding medium at high frequencies; it is rather that the radiation loading becomes that of radiation damping only.

As expected, when the shear modulus of the surrounding medium $\mu_m \to 0$ and $k_r \to \infty$, i.e. when the surrounding medium is a fluid, Eq. (10) shows that the torsional wavenumber $k_0^2 \to k_T^2$. Under these conditions the torsional wave is, as anticipated, uncoupled from the medium.

3. Radiation from the pipe to the ground surface

In the preceding analysis, we have included the effects of a surrounding medium on the axisymmetric torsional waves propagating in a buried pipe. However, the medium was considered to be of infinite extent, with no free surface being included in the analysis. Here, we wish to see how such waves

propagating in a buried pipe might radiate to a free surface and what resultant displacements might be seen at that surface. A comprehensive analysis of the fully coupled system, including the ground surface, would be extremely complex and beyond the scope of the present paper. What is offered here is a somewhat simplified analysis, in order to gain some understanding of the physical processes in play, and which makes the following assumptions:

- The effects of the soil on the pipe and the effects of the waves propagating in the pipe on the soil can be considered independently; what this means in practice is that, in the calculation of the dispersion characteristics of the torsional wave, the free ground surface (along with the concomitant wave reflections) is neglected – it is only included once the waves in the pipe have already, so to speak, been set up. Because of the large attenuation in most soils, this is only likely to become problematic at extremely low frequencies when the number of shear wavelengths between the pipe and the ground surface becomes very small.
- Once the waves radiating from the pipe reach the ground surface, they can be considered to be in the far field and undergo a plane wave treatment. This limits the lower frequency bound for which the analysis is valid, in a similar way to the assumption described above.
- Only excitation of the ground directly over the pipe is considered. Analytical description of the interaction of cylindrical and conical waves with a planar surface is complex. For example, at a lateral distance from the pipe axis comparable to the pipe depth, incident shear cylindrical or conical waves can excite surface waves of various kinds in addition to the reflected bulk waves [25, 26]. Directly over the pipe, which is the main region of interest for this study, surface waves do not develop, and only reflected shear waves need to be considered. A similar approach was adopted by Jette and Parker [27] when studying the effects on the ground surface of a fluid-borne wave propagating in a steel gas pipe.

For the torsional, n=0, s=0, wave propagating in a pipe, the excitation in the surrounding soil is given by Eqs. (2) and (8) as

$$u_\theta = \frac{V_s}{\mathrm{H}_1\left(k_{r0}^r a\right)} \mathrm{H}_1\left(k_{r0}^r r\right) e^{\mathrm{i}(\omega t - k_0 x)} \tag{16}$$

This equation represents conical shear waves radiating from the pipe into the soil. In the far field, for large values of $\left(k_{r0}^r r\right)$, this becomes [24]

$$u_\theta = \frac{V_s}{\mathrm{H}_1\left(k_{r0}^r a\right)} \sqrt{\frac{2}{\pi k_{r0}^r r}} e^{-\mathrm{i}\left(k_{r0}^r r - 3\pi/4\right)} e^{\mathrm{i}(\omega t - k_0 x)} \tag{17}$$

Eq. (17) shows that, in the far field, the incident wave field becomes quasi-planar, with a complex-exponential dependence moderated by the cylindrical spreading term. At this stage it is more convenient to adopt a Cartesian coordinate system in preference to a cylindrical one, with z denoting the direction normal to the ground surface, xy, plane, and the origin located on the pipe centre line. When the waves radiating from the pipe are incident upon the ground surface in the region directly above the pipe (now as plane waves), the travelling wave solutions for the soil displacements can now be expressed as

$$u_y = \left(V^+ e^{-\mathrm{i}k_{r0}^r z} + V^- e^{\mathrm{i}k_{r0}^r z}\right) e^{\mathrm{i}(\omega t - k_0 x)} \tag{18}$$

where the incident amplitude V^+ is given by

$$V^{+} = \frac{V_s}{\mathrm{H}_1\left(k_{r0}^{r}a\right)} \frac{\mathrm{i}-1}{\sqrt{\pi k_{r0}^{r} r}} \tag{19}$$

and the reflected amplitude V^- is to be determined by the boundary conditions at the ground surface.

At the ground surface, the condition that the shear stress is zero (σ_{zy}=0). Given that the vertical component of displacement at the ground surface is also zero, the shear stress is given by

$$\sigma_{zy} = \mu_m \frac{\partial u_y}{\partial z} \tag{20}$$

For a pipe buried at depth, *d*, this gives the reflected displacement amplitude V^- as

$$V^{-} = V^{+} e^{-2\mathrm{i}k_{r0}^{r}d} \tag{21}$$

i.e. a doubling of the response is seen at the free surface, analogous to the pure acoustic case. Substituting Eqs. (19) and (21) into Eq. (18) gives the soil displacement at the ground surface as

$$u_y\left(d\right) = \frac{2V_s}{\mathrm{H}_1\left(k_{r0}^{r}a\right)} \frac{\left(\mathrm{i}-1\right)}{\sqrt{\pi k_{r0}^{r} d}} e^{-\mathrm{i}k_{r0}^{r}d} e^{\mathrm{i}\left(\omega t - k_0 x\right)} \tag{22}$$

Eq. (22) relates the soil displacement at the surface, in the direction perpendicular to the pipe, to the circumferential displacement of the pipe shell wall directly beneath. The variation with frequency is not straightforward, with both the magnitude and the phase of the response at one location depending on the non-dimensional radial wavenumbers, $k_{r0}^{r}a$ and $k_{r0}^{r}d$. However, the solution presented above may be examined in a little more detail before recourse to numerical examples is required.

- At very low frequencies ($k_{r0}^{r}d < 1$), the solution presented is not valid as the waves at the ground surface cannot be considered plane.
- At high frequencies ($k_{r0}^{r}d > 1, k_{r0}^{r}a > 1$), adopting the large argument approximation for the Hankel function, Eq. (22) becomes

$$u_y\left(d\right) = 2V_s \sqrt{\frac{a}{d}} e^{-\mathrm{i}k_{r0}^{r}\left(d-a\right)} e^{\mathrm{i}\left(\omega t - k_0 x\right)} \tag{23}$$

  This shows that here the pipe behaves as a plane wave source with the plane waves following a cylindrical spreading law.
- At mid frequencies ($k_{r0}^{r}d > 1, k_{r0}^{r}a < 1$) the full form of Eq. (22) must be employed.

The numerical examples presented in the following section serve to illustrate the expected behaviour in a variety of situations.

4. Example results

Examples are presented for a typical cast iron pipe buried in two soil types, representing a sandy soil and a clay soil, respectively. The relevant pipe and soil parameters are shown in Table 1.

	Pipe	Sandy soil	Clay soil
Density (kg/m^3)	7800	2000	2000
Shear modulus (GN/m^2)	65	0.02	0.18
Poisson's ratio	0.2		
Loss factor	0.001	0.1	0.1
Pipe thickness/radius	0.1		
Pipe depth/radius	10		

Table 1
Pipe and soil elastic properties

4.1. Analytical dispersion relationships

Figs. 2(a) and (b) show the real parts of the wavenumber and the wave attenuation (presented as loss in dB per unit propagation distance - measured in pipe radii) respectively for both types of pipe in each soil. For the real parts (Fig. 2a), the *in-vacuo* values are also shown; for the imaginary parts, the high frequency approximations given by Eq. (15) are included. Eq. (11) is used in order to present the results in non-dimensional form; the non-dimensional wavenumbers are plotted against the free-field non-dimensional wavenumber for water, $k_f a$. (Note that, for a pipe of radius 100mm, the maximum frequency presented in the figures is approximately 5kHz, with the ring frequency being approximately 7.3kHz. Furthermore, the ring frequency will occur at a value of $k_f a \approx 3$, regardless of the pipe radius.) It should also be noted that, as for the s=1, 2 wavetypes, the solutions to Eq. (11) must be found recursively, also using the relationship $(k_{r0}^r)^2 = k_r^2 - k_0^2$; moreover, a choice must be made as to the sign of the square root of $(k_{r0}^r)^2$. Here, the choice is made based on the assertion that the pipe waveumber, k_0, must have a negative imaginary part, so that waves travelling along the pipe decay, rather than grow (this differs slightly from the s=1, 2 cases presented previously in that, for these, both choices of square root resulted in a decaying pipe wave, so a further constraint was required in order to decide which root should be used).

Fig. 2(a) shows that the real part of the wavenumber (and hence the wavespeed) is very close to the *in-vacuo* value at all the frequencies considered, for both soil types. Even at low frequencies, the effect of the soil is small. Close inspection reveals there to be a very slight decrease in the values relative to the *in-vacuo* case, with this effect being slightly greater in the clay soil. This indicates that, the soil exerts a small stiffness effect on the pipe. Moreover, the wavenumber curve does not pass through the origin, suggesting that the wavespeed tends to zero at very low frequencies and that the wave may be cut-off.

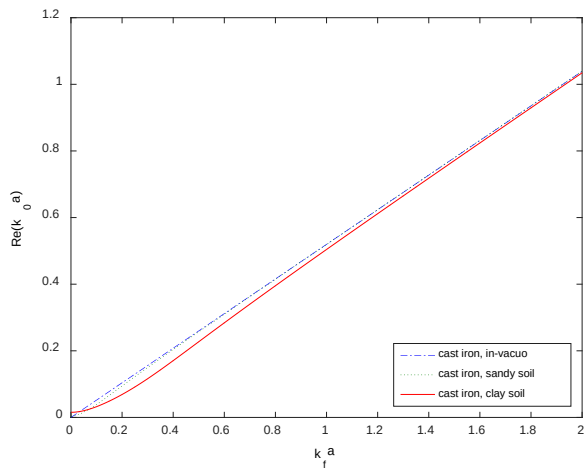

(a)

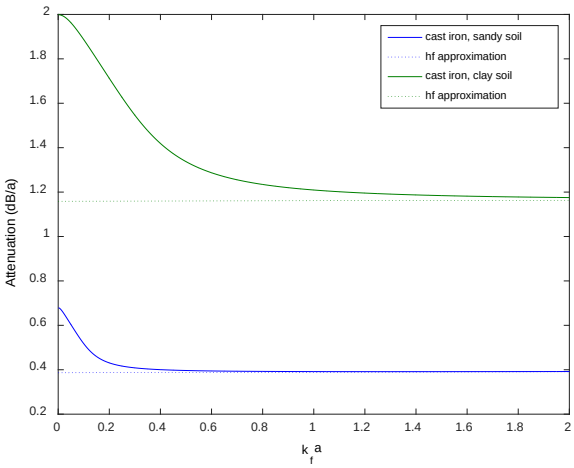

(b)

Fig. 2. Predicted wavenumbers for cast iron pipe buried in sand/clay: (a) real part; (b) attenuation.

Wavenumbers were also computed assuming no loss in the soils, in order to evaluate the effect of the soil damping. As anticipated, it was found that the soil damping had a negligible effect on the real part of the wavenumbers.

Fig. 2(b) shows that, for the cast iron pipe, the wave attenuation is of the order of 1-2dB/a at low frequencies and decreases with frequency, reaching the constant value predicted by Eq. (15). The attenuation is larger for the clay soil, as might be expected, given the higher shear stiffness of clay. As for the real part of the wavenumber, the effect of soil damping on the wave attenuation was found to be extremely small for both pipe/soil combinations.

4.2. Response at the ground surface

Figs 3(a) and (b) show the displacement response at the ground surface relative to the pipe wall displacement, for each type of soil. The responses presented are derived from Eq. (22); the approximate responses at high frequency, given by Eq. (23) are also included. Frequencies for which data are considered invalid, by virtue of the responses not being in the far field, have been excluded from the plots. Examining Fig 3(a), it can be seen that the response is consistently less at the ground surface than on the pipe, becoming a linear variation at higher frequencies. This is as might be expected, given that the waves undergo both attenuation due to soil damping and cylindrical spreading in order to reach the surface. Here, large differences between the two soil types can be seen, with the attenuation in the clay soil being much less than in the sandy soil. This is largely due to the soil damping itself which has a much greater effect on the smaller wavelengths present in the sandy soil compared with those propagating in the clay soil. Almost none of the frequency range has been excluded for not meeting the far field condition at the surface, suggesting that the non-dimensional wavenumber, $k_0^r d$, is greater than unity even at very low frequencies. This, again, is as expected, given that the wavenumber in the pipe approximates the *in-vacuo* value and, in turn, is much smaller than the free-field wavenumber in the soil. For both the cases considered, the high frequency approximations are valid for all but very low frequencies.

Fig. 3(b) shows the phase of the ground surface displacement relative to that seen on the pipe wall. Again, the differences result from the phase lag of a wave travelling a certain distance along the pipe compared with a wave travelling a longer distance in the surrounding soil. The high-frequency approximations are, here, indistinguishable from the full solution over the whole frequency range.

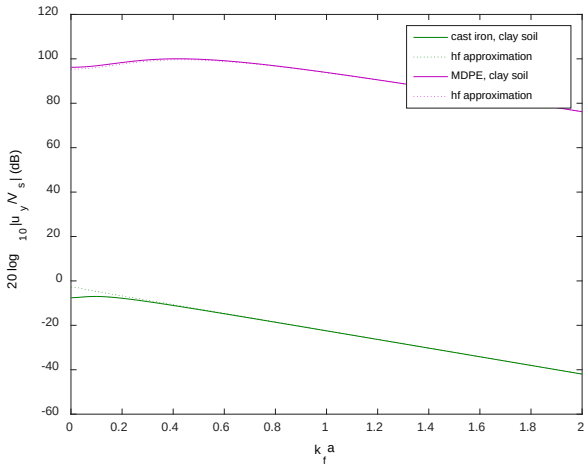

(a)

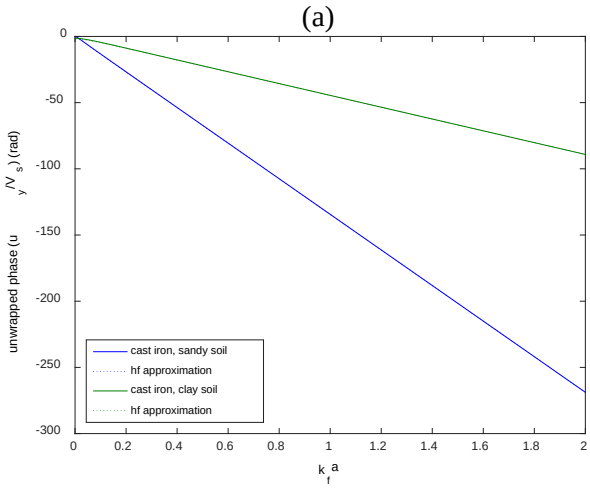

(b)

Fig. 3. Displacement response at ground surface, relative to pipe wall displacement for cast iron pipe buried in sand/clay: (a) magnitude (dB); (b) unwrapped phase (rad).

5. Discussion and Conclusions

In this paper, axisymmetric torsional wave motion in a buried pipe has been studied. At the pipe/soil interface, compact contact has been assumed, for which continuity of circumferential displacement is maintained. An analytical dispersion relationship has been derived for the n=0, s=0, torsional wave. This wave is uncoupled from any contained fluid but, for the purposes of deriving the dispersion relationships, a surrounding medium of infinite extent was presumed. These expressions, along with low and high-frequency approximations, permitted insights to be gained into the physical mechanisms at play. Furthermore, expressions were derived for the ground surface displacement directly above the pipe, resulting from torsional wave motion within the pipe wall. Numerical examples were then presented.

It was found that, for the cast iron pipe considered here, the effect of the soil (for either soil type) on the real part of the wavenumber, and hence wavespeed, was small. The small differences between the soil-loaded cases and the *in-vacuo* case demonstrated that, at low frequencies, the soil exerts a small stiffness effect. Contrastingly, the effect of the surrounding soil on the wave attenuation can be considerable.

The torsional wave propagating in a buried pipe will radiate into the surrounding soil purely as a shear wave, which might be detectable at the ground surface. For the cast iron pipe studied here,

detection at the ground surface might be possible. In particular, for pure torsional motion in an ideal medium, the resulting displacement at the ground surface directly above the pipe is confined to one direction: perpendicular to the pipe and in the plane of the surface. This is in contrast to the ground surface displacements resulting from either s=1 (fluid-dominated) or s=*2* (shell-dominated) axisymmetric wave motion in the pipe; under ideal conditions these displacements are confined to being a combination of vertical and horizontal, in-line with the pipe [28]. These differences may be brought to bear when attempting to determine, from the ground surface, which type of wave motion has occurred in the pipe, for example when a fracture event occurs.

Monitoring torsional waves directly on the pipe may also be beneficial, and not only for detecting the presence or not of torsional wave motion. As stated earlier, the n=0, s=0 torsional wave, such as is described in this paper, is frequently exploited for the detection of faults and cracks in pipes, see for example [15-22]. Mainly carried out at ultrasonic frequencies, inspections of this sort are possible because, at high frequencies, the wave is non-dispersive; moreover, the attenuation is atypically low and invariant with frequency in this frequency regime. The investigations presented here show that these trends do, in fact, persist at much lower frequencies, well into the audible range. Knowledge of this would allow pipe inspections to be carried out at these lower frequencies. Whilst the disadvantages of this approach are immediately apparent (the scale of the faults would need to be much greater and the excitation devices correspondingly larger), there would also be advantages of monitoring torsional waves in this way: sampling rates on acquisition and analysis equipment could be much lower, thus potentially reducing costs dramatically; larger, potentially more catastrophic, defects could be more readily exposed (more important, perhaps where repair and replacement prioritization is an issue, such as in the water industry); and finally, leak detection equipment generally operates in the audible frequency range so possibilities might open up for incorporating torsional wave monitoring into existing equipment.

The findings presented here open up new possibilities for both pipe damage detection and for the remote detection of pipe fracture in cast iron pipes, at audio frequencies. Future work will address whether such approaches are viable in practice.

Acknowledgements

The authors gratefully acknowledge the support provided by the EPSRC (under grant EP/K021699/1).

References

[1] www.mappingtheunderworld.ac.uk
[2] www.assessingtheunderworld.org
[3] A.C.D. Royal, P.R. Atkins, M.J. Brennan, D.N. Chapman, H. Chen, A.G. Cohn, K.Y. Foo, K. Goddard, R. Hayes, T. Hao, P.L. Lewin, N. Metje, J.M. Muggleton, A. Naji, G. Orlando, S.R. Pennock, M.A. Redfern, A.J. Saul, S.G. Swingler, P. Wang, C.D.F. Rogers, Site assessment of multiple-sensor approaches for buried utility detection, *International Journal of Geophysics* (2011) (Article ID 496123).
[4] J.M. Muggleton, E. Rustighi, 'Mapping the Underworld': recent developments in vibro-acoustic techniques to locate buried infrastructure, *Géotechnique Letters* 3 (July-September) (2013) 137-141.
[5] M. Fantozzi, G.D. Chirico, E. Fontana, F. Tonolini, Leak inspection on water pipelines by acoustic emission with cross-correlation method, *Annual Conference Proceeding, American Water Works Association, Engineering and Operations*, San Antonio, Texas, USA, 1993.
[6] H.V. Fuchs, R. Riehle, Ten years of experience with leak detection by acoustic signal analysis, *Applied Acoustics* 33(1) (1991) 1-19.
[7] D.A. Liston, J.D. Liston, Leak detection techniques, *Journal of the New England Water Works Association* 106(2) (1992) 103-108.
[8] J.M. Makar, R. Desnoyers, S.E. McDonald, Failure modes and mechanisms in gray cast iron pipe. *NRC Report*, NRCC-44218, 2001, www.nrc.ca/irc/ircpubs.

[9] O. Hunaidi, W.T. Chu, Acoustical characteristics of leak signals in plastic water distribution pipes, *Applied Acoustics* 58 (1999) 235-254.
[10] J.M. Muggleton, M.J. Brennan, R.J. Pinnington, Wavenumber prediction of waves in buried pipes for water leak detection, *Journal of Sound and Vibration* 249(5) (2002) 939-954.
[11] J.M. Muggleton, M.J. Brennan, P.W. Linford, Axisymmetric wave propagation in fluid-filled pipes: wavenumber measurements *in-vacuo* and buried pipes, *Journal of Sound and Vibration* 270(1–2) (2004) 171-90.
[12] J.M. Muggleton, M.J. Brennan, Leak noise propagation and attenuation in submerged plastic water pipes, *Journal of Sound and Vibration* 278 (2004) 527-537.
[13] J.M. Muggleton, J. Yan, Wavenumber prediction and measurement of axisymmetric waves in buried fluid-filled pipes: inclusion of shear coupling at a lubricated pipe/soil interface, *Journal of Sound and Vibration* 332 (2013) 1216-1230.
[14] Y. Gao, F. Sui, J.M. Muggleton, J. Yang, Simplified dispersion relationships for fluid-dominated axisymmetric wave motion in buried fluid-filled pipes, Submitted to *Journal of Sound and Vibration*, 2015 .
[15] T.K. Lockett, Lamb and torsional waves and their use in flaw detection in tubes, *Ultrasonics* 11(1) (1973) 31-37.
[16] A. Løvstad, P. Cawley, The reflection of the fundamental torsional guided wave from multiple circular holes in pipes, *NDT & E International* 44(7) (2011) 553-562.
[17] R. Kirby, Z. Zlatev, P. Mudge, On the scattering of torsional elastic waves from axisymmetric defects in coated pipes. *Journal of Sound and Vibration* 331(17) (2012) 3989-4004.
[18] R. Carandente, P. Cawley, The effect of complex defect profiles on the reflection of the fundamental torsional mode in pipes, *NDT & E International* 46 (2012) 41-47.
[19] A. Løvstad, P. Cawley, The reflection of the fundamental torsional mode from pit clusters in pipes, NDT & E International 46 (2012) 83-93.
[20] E. Leinov, M.J.S. Lowe, P. Cawley, Investigation of guided wave propagation and attenuation in pipe buried in sand, *Journal of Sound and Vibration* 347(7) (2015) 96-114.
[21] Y.E. Kwon, H.W. Kim, Y.Y. Kim, High-frequency lowest torsional wave mode ultrasonic inspection using a necked pipe waveguide unit, *Ultrasonics* 62 (2015) 237-243.
[22] Z. Liu, C. He, B. Wu, X. Wang, S. Yang. Circumferential and longitudinal defect detection using T(0, 1) mode excited by thickness shear mode piezoelectric elements, *Ultrasonics* 44(Supplement) (2006) 1135-1138.
[23] E. H. Kennard, The new approach to shell theory: circular cylinders, *Journal of Applied Mechanics* (1953) 33-40.
[24] M. Abramowitz, I.A. Stegun, *Handbook of Mathematical Functions*, Dover publications, New York, 1965.
[25] W.M. Ewing, W.S. Jardetzky, F. Press, *Elastic Waves in Layered Media*, New York: McGraw-Hill, 1957.
[26] A.N. Jette, J.G. Parker, Excitation of an elastic half-space by a buried line source of conical waves, *Journal of Sound and Vibration* 67 (1979) 523-531.
[27] A.N. Jette, J.G. Parker, Surface displacements accompanying the propagation of acoustic waves within an underground pipe, *Journal of Sound and Vibration* 69(2) (1980) 265-274.
[28] Y. Gao, J.M. Muggleton, E. Rustighi, J. Yang, J. Tian, Ground surface vibration due to axisymmetric wave motion in buried fluid-filled pipes, *Proceedings of the 22nd International Congress on Sound & Vibration, ICSV22*, Florence, Italy, 2015.